Turkish Journal of Electrical Engineering & Computer Sciences

http://journals.tubitak.gov.tr/elektrik/

Research Article

Turk J Elec Eng & Comp Sci
(2014) 22: 1099 – 1115

doi:10.3906/elk-1212-39

Stability analysis of multimachine thermal power systems using the nature-inspired modified cuckoo search algorithm

Shivakumar RANGASAMY*, Panneerselvam MANICKAM
Sona College of Technology, Salem, Tamil Nadu, India

Received: 07.12.2012 • **Accepted:** 15.02.2013 • **Published Online:** 15.08.2014 • **Printed:** 12.09.2014

Abstract: The stability of modern interconnected thermal power systems is greatly affected by the presence of low-frequency inertial oscillations in the system, due to various forms of disturbances experienced. This paper provides an efficient damping solution to these oscillations based on nature-inspired modified cuckoo search algorithm-based controller design. The proposed controller design is formulated as a parameter optimization problem based on damping ratio and time-domain error deviations. The effectiveness of the proposed damping controller design is illustrated by performing the nonlinear time domain simulations of the test multimachine power systems under various operating conditions and disturbances. Moreover, an exhaustive comparative stability analysis is performed based on the damping performance of the modified cuckoo search controller design over the genetic algorithm-based and cuckoo search algorithm-based controller designs.

Key words: Low-frequency inertial oscillations, damping ratio, nature-inspired optimization, cuckoo search algorithm, multimachine thermal systems

1. Introduction

The stable operation of modern interconnected power systems is becoming more complex due to various forms of instabilities [1]. The concept of angular stability in power systems has received a great deal of attention in recent years. Angular instability is mainly responsible for causing low-frequency inertial oscillations in power system networks. These low-frequency oscillations are alternator rotor angle oscillations with a frequency range of around 2 Hz and these are considered to be the most important root cause for blackouts in interconnected power systems [2,3].The implementation of a power system damping controller (PSDC) in power system networks is the most cost-effective method for the mitigation of these oscillations. The main function of the PSDC is to provide positive damping to these oscillations using supplementary stabilizing signals. The effectiveness of the PSDC depends upon its tuning phenomenon. The parameters of the PSDC must be tuned using a robust algorithm so that a global optimal solution will be achieved for better system stability. Tuning of the PSDC using conventional algorithms will lead to a local optimum solution that is not sufficient for system stability.

Conventional damping controllers designed using the lag-lead theory can provide good damping to these oscillations at a particular operating condition [4,5]. However, the damping performance of these controllers will not be satisfactory for other operating conditions and network changes. Since modern interconnected power systems are highly dynamic, it is the responsibility of the power system operator to design an adaptive controller, which can be tuned to provide effective damping at all possible variations in the system. Damping controllers

*Correspondence: mukilvarshan@gmail.com

were designed and implemented using the concepts of neural networks, fuzzy logic, variable structure control, and adaptive algorithms in [6–8]. These controllers gave effective damping suitable for system stability, but these controllers had some disadvantages with respect to complex design procedures in fuzzy logic, difficulty in training the neural network, etc. [9].

Recently, as an alternative to these techniques, nature-inspired optimization algorithms were extensively implemented in various engineering optimization problems. These include evolutionary programming, harmony search algorithm, honey bee algorithm, genetic algorithm (GA), particle swarm optimization (PSO), shuffled frog leaping algorithm, cuckoo search (CS) algorithm, self-adaptive differential evolution (JDE) algorithm, adaptive differential evolution (JADE) algorithm, strategy adaptation-based differential evolution (SADE) algorithm, and differential search algorithm (DSA) [10–15]. These algorithms can be implemented effectively to solve complex power system parameter optimization problems.

In this paper, the GA, CS, and proposed modified CS (MCS) algorithms are implemented for the controller design, so that optimal controller parameters can be computed for better stability of the system. The main objective of this paper is to damp the low-frequency inertial oscillations experienced in the test IEEE 3-machine 9-bus and IEEE 10-machine 39-bus multimachine thermal power systems and to enhance the stability of these systems using various nature-inspired damping controller designs, namely the GAPSDC, CSPSDC, and MCSPSDC. The design problem is formulated as a parameter optimization problem with objective functions based on damping ratio and time-domain error deviations.

The optimal controller parameters computed using the 3 damping controller designs are implemented in closed-loop modeling of the systems to compute the damping ratios of the system. A detailed comparative stability analysis is done based on the damping performance of the 3 controllers under various operating conditions and parameter changes. The simulation results of the test multimachine systems prove the robustness of the proposed MCS algorithm-based controller design. The damping performance in terms of the damping ratio maximization and error deviation minimization are better for the proposed MCSPSDC in comparison with GAPSDC and CSPSDC. The proposed MCSPSDC design can be implemented for modern complex interconnected power system networks, so that the experienced low-frequency inertial oscillations will be effectively damped to enhance the power system stability.

2. Problem statement

2.1. Modeling of the test power systems

In the case of multimachine system modeling, the following assumptions are implemented in this paper.

1. The mechanical power input (governor turbine) variations are included in the modeling.
2. Natural damping (D, due to damper windings) in the system is assumed to be very negligible.
3. The generator is modeled as a constant voltage source behind a transient reactance.

The effect of thermal governor-turbine dynamics is included in the modeling of the multimachine system along with the synchronous generator model. This is an important feature of this work, since the mechanical power input variations (governor turbine effect) are taken as constants in the classical model of power system stability analysis. The proposed controllers will damp both the torsional mode and intra mode of oscillations in the system considered. The torsional mode of oscillations will be due to the interaction of the governor-turbine variations with generator-excitation system variations.

Two test multimachine power systems are taken for modeling and simulation in this paper. Figure 1 represents the IEEE 3-machine 9-bus thermal power system and Figure 2 represents the IEEE 10-machine 39-bus power system network. All of the system data and specifications are given in Appendix A [16,17].

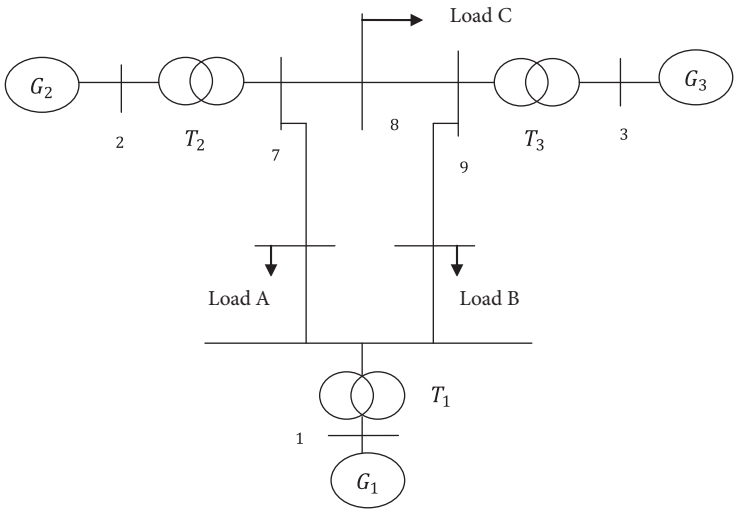

Figure 1. IEEE 3-machine 9-bus power system model.

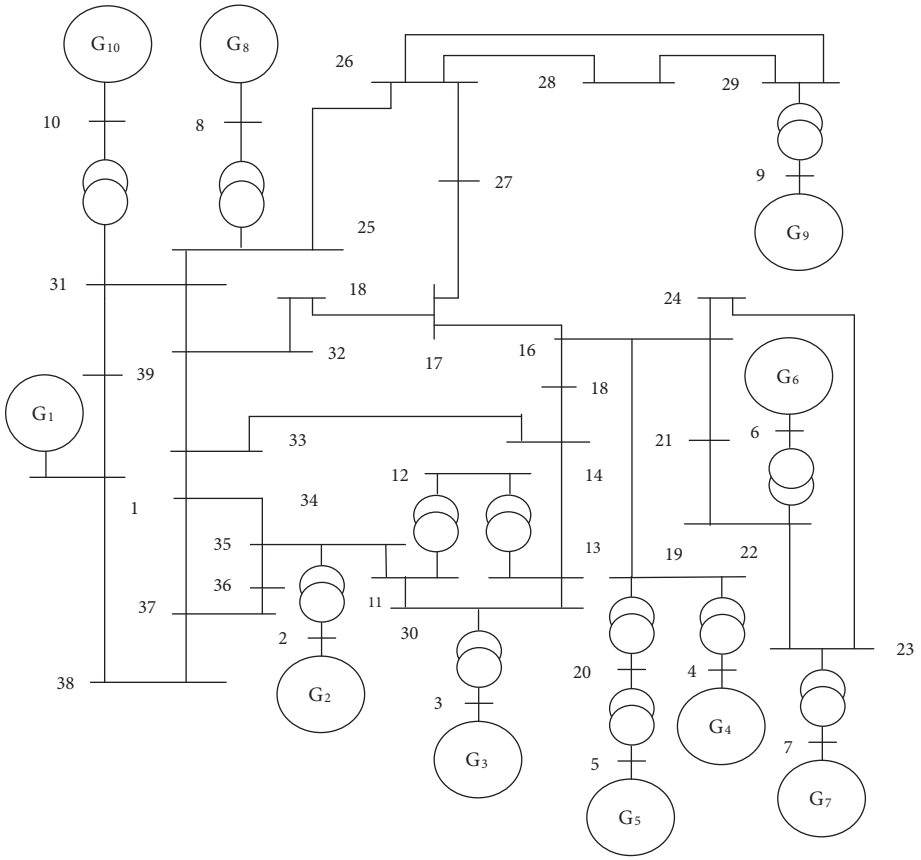

Figure 2. IEEE 10-machine 39-bus power system model.

Figure 3 represents the Heffrons–Phillips synchronous generator model taken for the state space modeling and analysis of the system [18]. The PSDC in this model represents the PSDC implemented in the generator excitation system feedback loop.

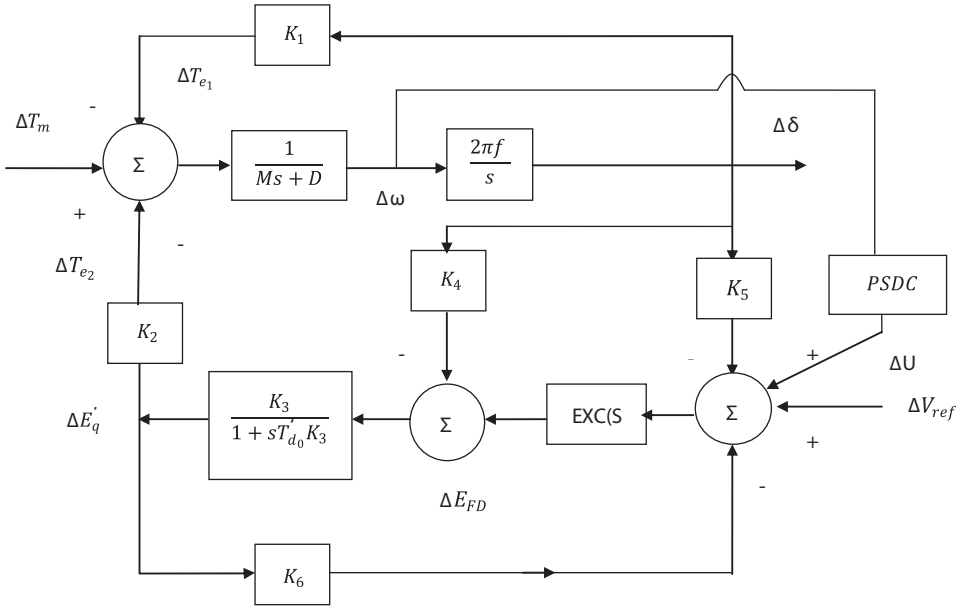

Figure 3. Heffron–Phillips generator model with a controller.

The dynamic linearized state space equation used for modeling the power systems is given by:

$$[\dot{x}] = Ax + Bu, \tag{1}$$

where x is the state variable vector taken for modeling, and A and B are the state matrix and input matrix, respectively.

In this paper, 2 types of thermal system configurations (the S_A and S_B models) are implemented in the modeling and stability analysis.

S_A model: For this model, the generator is modeled with a rotating-type IEEE type 1 excitation system along with the effect of thermal governor- and reheat-type turbines.

S_B model: For this model, the generator is modeled with a static-type IEEE ST1A excitation system along with the effect of thermal governor- and nonreheat-type turbines.

Figure 4 represents the S_A model, in which the thermal governor and reheat turbine with reheat time constant T_{RH} are included along with the Heffrons generator model for modeling and analysis. Figure 5 represents the IEEE type 1 excitation system model implemented in the S_A model.

Figure 6 represents the thermal S_B model, in which the thermal governor and nonreheat turbine with time constant T_T are included along with the Heffrons generator model for modeling and analysis. Figure 7 represents the IEEE ST1A excitation system model implemented in the S_B model.

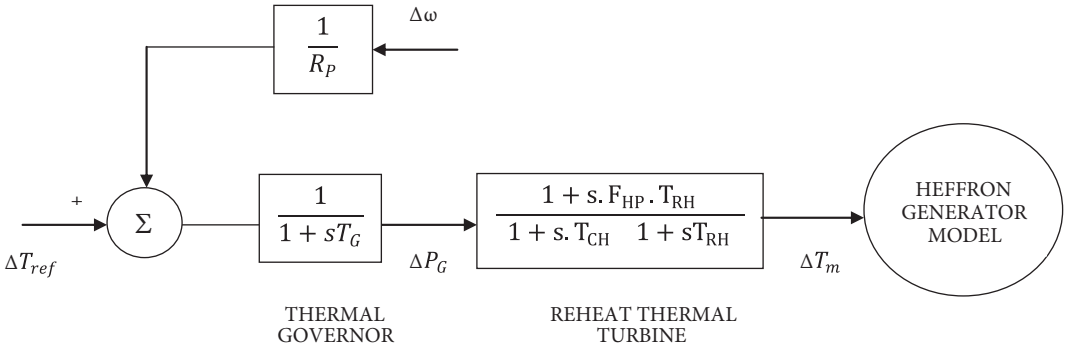

Figure 4. S_A thermal system model.

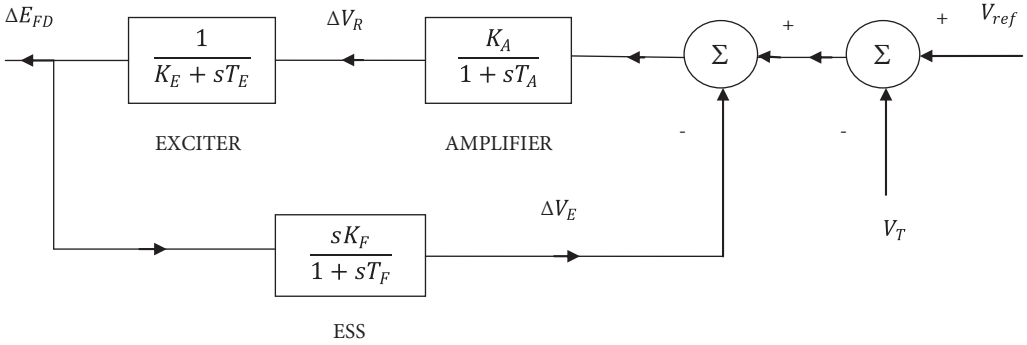

Figure 5. IEEE type 1 excitation system model.

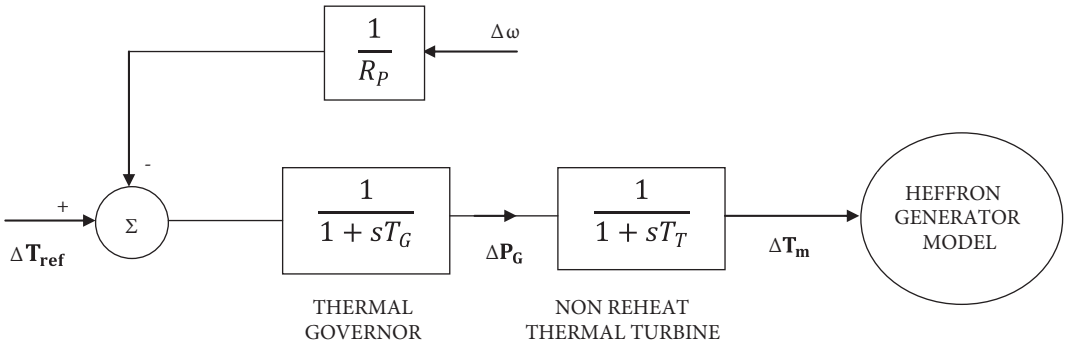

Figure 6. S_B thermal system model.

Figure 8 represents the PSDC model. It consists of the reset block, gain K_S block, and the 2-stage phase compensation block. The input to the PSDC is the rotor speed deviation ($\Delta\omega$) and the output is the damping control signal (ΔU) given to the generator-excitation system feedback loop. The purpose of the PSDC is to provide positive damping torque to the rotor inertial oscillations, thereby improving stability of the system.

2.2. State space modeling of the S_A and S_B models

The following are the state variables selected for the state space modeling of thermal system models:

$$[x_{SA}]_{CLOSED} = [\Delta\omega, \Delta\delta, \Delta Eq', \Delta E_{FD}, \Delta V_R, \Delta V_E, \Delta P_G, \Delta Tm, \Delta S_1, \Delta S_2, \Delta U]^T, \tag{2}$$

$$[x_{SB}]_{CLOSED} = [\Delta\omega, \Delta\delta, \Delta Eq', \Delta E_{FD}, \Delta V_E, \Delta P_G, \Delta Tm, \Delta S_1, \Delta S_2, \Delta U]^T. \quad (3)$$

Eqs. (2) and (3) represent the closed-loop state variables for the S_A and S_B models, respectively. The closed-loop state matrix order will be (11 × 11) for the S_A model and it will be (10 × 10) for the S_B model. ΔS_1, ΔS_2, and ΔU are the state variables selected from the PSDC model. The various abbreviations and variables used in this paper are given in Appendix B.

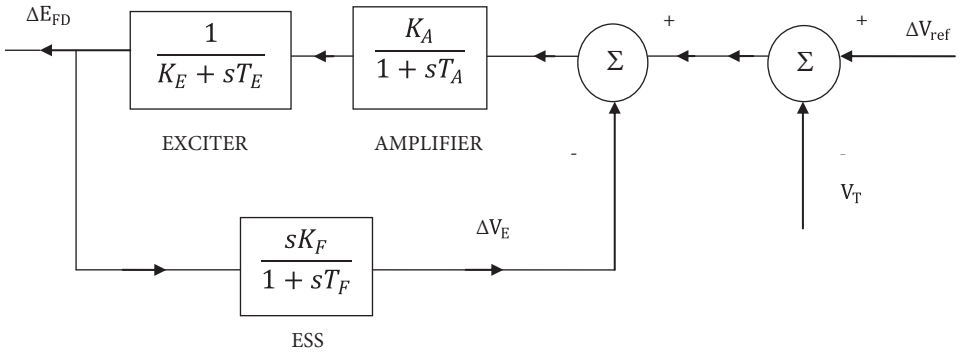

Figure 7. IEEE ST1A excitation system model.

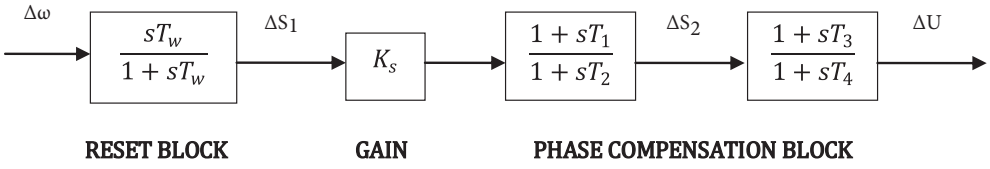

Figure 8. PSDC model.

3. Proposed optimization criterion and PSDC tuning

The primary aim of this proposed optimization criterion is to compute the global optimal solution required for stability of thermal power systems. The proposed tri-objective optimization criterion consists of 2 objective functions (J_A and J_B).

3.1. Objective function J_A

The magnitude of damping provided to a practical power system is represented in terms of the damping ratio. The damping ratio can be calculated from the computed system eigenvalue. The objective function J_A is set to a minimum of ξ_k among the damping ratios of the electromechanical modes of oscillation, as given in Eq. (4).

$$J_A = Min(\xi_k). \quad (4)$$

Here, ξ_k belongs to a computed set of electromechanical modes of oscillation for a particular operating condition. ξ_k represents the damping ratio of the kth electromechanical mode eigenvalue. The aim here is to maximize the damping ratio of the weakly damped oscillatory eigenvalue for better stability.

3.2. Objective function J_B

The system electromechanical oscillations are reflected in terms of the rotor speed and power angle deviations. The damping of oscillations involves minimizing the deviations of the rotor speed and power angle involved in the system.

$$J_B = \int_0^T e^2(t) \cdot dt \tag{5}$$

The objective here is to minimize [J $_B$], so that the integral of the squared error deviations in the rotor speed and power angle are minimized for better stability of the system, i.e. to minimize the deviation overshoots and settling time of the deviations as early as possible. The optimization problem, including the proposed constraints, is formulated as follows:

Optimize J [Maximize J $_A$, Minimize J $_B$]

Subject to

$$T_1^{\min} \le T_1 \le T_1^{\max} \quad K_S^{\min} \le K_S \le K_S^{\max} \tag{6}$$

$$\mathrm{Ks}^{\min} \le \mathrm{Ks} \le Ks^{\max} \tag{7}$$

$$P_x^{\min} \le P_x \le P_x^{\max} \tag{8}$$

$$T_2^{\min} \le T_2 \le T_2^{\max} \tag{9}$$

$$\alpha^{\min} \le \alpha \le \alpha^{\max} \tag{10}$$

Here, Eqs. (3) to (6) represent the constraints taken in the optimization problem to compute the global solution suitable for stability of the system.

3.3. PSDC tuning

The PSDC is tuned effectively using the proposed controller design algorithm. Ks, T $_1$, and T $_2$ are the parameters involved in the PSDC. P $_X$ and α will be discussed in detail with respect to the MCS algorithm in Section 4.2 of this paper. The lower and upper limits of these 5 parameter constraints are given in Appendix A.

4. Proposed MCS algorithm for stability

4.1. An overview of the conventional CS algorithm.

The CS algorithm was developed by Yang and Deb in 2009 [19]. This algorithm is best suited to complex optimization problems and its performance is better when compared to other nature-inspired algorithms like the GA, PSO, etc. [20,21].

The CS algorithm was inspired by the interesting natural breeding of the cuckoo species [22]. Cuckoo species lay their eggs in the nests of other host birds. The host birds often have conflict with the cuckoos. Whenever the host bird finds that the eggs are of alien type, they immediately throw all of the alien eggs out of their nests. Some host birds will destroy their nests and build a new nest some other place.

Another feature of these cuckoo species is that parasitic cuckoos will choose a nest where the host bird laid its own eggs. Whenever the first cuckoo chick is hatched, the host eggs will be evicted from the nests by the cuckoos. This will increase the share of food for the cuckoo chicks.

Generally, the following points are implemented for implementing the CS algorithm.

- Each cuckoo will lay one egg at a time. It will dump this egg in a randomly chosen nest.
- The nests with eggs of higher quality will be carried on to the next generation for finding better solutions.
- The available host nests ('n' nests) are taken as constants. The host bird will find the alien egg in the nest with a probability Px.

The breeding behavior of the cuckoo species is based on Levy flights. Levy flight is nothing but the random walk performed by animals in nature in search of food. When generating new solutions $x^{(t+1)}$, a Levy flight is performed based on Eq. (11).

$$x_i^{(t+1)} = x_i^{(t)} + \alpha(t^{-\lambda}). \tag{11}$$

Here, α is the step size and λ will have values from 1 to 3.

The above concepts are incorporated into the implementation of the CS algorithm for finding the global optimal solution required for stability of the system.

4.2. Proposed MCS algorithm

In the proposed MCS algorithm, the shortcomings experienced in the conventional CS algorithm are modified to obtain an effective solution, suitable for thermal power system stability.

In the conventional CS algorithm, the worst nest's probability Px and step size α used in the algorithm are taken as constants. In light of this, the number of iterations required for an optimal solution is large. The performance of the algorithm will be poor, leading to a higher number of iterations, whenever the value of Px is low and the value of α is large. Moreover, a higher Px value and lower α value will not provide the best solution suitable for better stability.

Based on the above demerits, the proposed MCS algorithm will solve the above problem by taking the probability Px and step size α as constraints in the proposed optimization problem discussed in Section 3.2 and Eqs. (6) and (11). The proposed modified algorithm will select an optimal value for probability Px and α at the final iteration along with the optimal solution for the PSDC parameters Ks, T1, and T2. In the MCS algorithm, the following limits are selected for Px and α. For Px, the range is between 0.001 and 1, and for α, it is between 0.01 and 0.6.

Figure 9 represents the pseudocode for the proposed MCS algorithm to obtain the optimal parameters required for better stability. In this code, g represents the generation number and gmax represents the maximum number of generations.

The proposed MCS algorithm implemented in this paper to obtain the optimal damping controller parameters is given as follows:

Step 1: Specify the various parameters involved for the MCS algorithm implementation (i.e. number of host nests, limits for the PSDC parameters (Ks, T_1, and T_2), worst nest's probability, step size, number of generations, termination criteria, etc.).

Step 2: Initialize a population of n host nests in the problem space of the possible solutions.

Step 3: Compute the fitness function (Pi) for the randomly selected cuckoo (i) by Levy flights.

Step 4: Choose a nest k among available nests and replace k by new solution, if the fitness (Pi) is greater than fitness (P_k).

Step 5: If the termination condition is reached, then optimal solution is equal to those obtained in current generation; otherwise, go to step 6.

```
begin MCS

        g=1;
        Initialize population with n host nests;
        Compute the fitness P(i) for selected cuckoo (i);
        Choose a nest k among available n nests;

        If (P i > P k),
        Replace k by a new solution;
        end

    While (g > g max ) not done do

        Abondon a fraction of worst nests with P x and step size α,
        Update the solutions to compute optimal K s, T 1, T 2, P x, α;
    end While

end MCS.
```

Figure 9. Pseudocode for the proposed MCS algorithm.

Step 6: Abandon a fraction of the worse nests with the optimal value of probability Pa and step size α.

Step 7: Update the solutions to calculate $x_i^{(t+1)}$, using Eq. (11).

Step 8: Repeat steps 3–7 until the termination criterion is met.

4.3. An overview of the GA

In this paper, the damping performances of the CS algorithm-based and MCS algorithm-based controller designs are compared with the GA-based controller design. GAs are nature-inspired algorithms inspired by natural selection and genetics [23–25]. The following 4 operators are essential in the GA to create the fittest individuals: selection, crossover, mutation, and replacement.

Selection is the process of identifying 2 parent chromosomes from the initial population for reproduction. The roulette wheel selection concept is implemented in this paper. The roulette wheel selection is a genetic selection operator for selecting potentially useful solutions for recombination compared to other selection methods.

Crossover is the process of taking 2 selected parent chromosomes to produce better offspring. In this work, the uniform crossover method is implemented. After the crossover, the strings are subjected to the phenomenon of mutation. Mutation recovers the lost genetic materials involved in the genetic process. Mutation of a bit involves flipping a bit, i.e. changing 0 to 1 and vice versa.

Replacement is the last stage in the genetic cycle. In this paper, weak parent replacement involving a generation gap of 0.8 is implemented.

5. Simulation results and stability analysis

The MATLAB tool is implemented for the modeling and simulation of the test multimachine power systems in this paper. The system data used for simulation are given in Appendix A.

5.1. Three-machine 9-bus system results.

In the 3-machine test system, the 125-MVA generator bus is taken as the infinite bus and the system is considered with generators G_2 and G_3 providing power to the infinite bus. Table 1 represents the generator loading conditions, with ΔPd being the load change disturbance given to the system. The linearized state space modeling of the test system provides the open-loop eigenvalues, as given in Table 2. The damping ratios are calculated for the weakly damped oscillatory mode eigenvalues. The complex eigenvalues with negative real parts represent the decaying mode of oscillations. The weakly damped eigenvalue is identified among the complex eigenvalues computed for a particular operating condition. The negative damping ratios in Table 2 indicate that the system is unstable. Moreover, the speed deviation response in Figure 10 indicates that the deviations are more oscillatory, leading to instability. In order to make the system stable, damping controllers are to be implemented using the 3 nature-inspired algorithms.

Table 1. Generator loading conditions for the 3-machine test system.

Generator	Case A		Case B	
	P (p.u)	Q (p.u)	P	Q
G1	0.72	0.27	2.21	1.09
G2	1.03	0.07	1.92	0.56
G3	0.85	–0.11	1.28	0.36
Load disturbance	ΔPd = 0.02 p.u		ΔPd = 0.04 p.u	

Table 2. Computed open-loop eigenvalues and damping ratios without PSDC.

S. No.	Operating conditions (p.u)	Weakly damped values	
		Eigenvalues	Damping ratios
1	Case A	0.0241 ± j 5.141	–0.004687
2	Case B	0.019 ± j 4.711	–0.004033

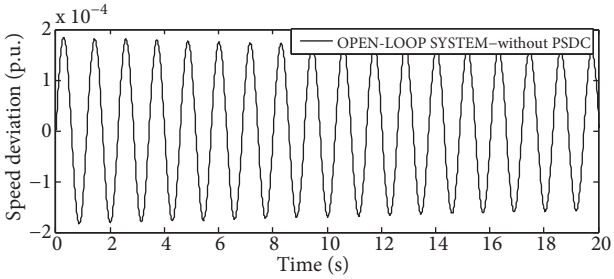

Figure 10. Speed deviation response of the open-loop system for Case A conditions.

5.2. Proposed MCS algorithm implementation

The 3 algorithms (GA, CS, and MCS) are implemented to compute the optimal parameters, Ks, T_1, T_2, Px, and α. These optimal values are substituted in the closed-loop modeling of the test systems considered to compute the closed-loop eigenvalues and damping ratios. Table 3 provides the various parameters selected for algorithm implementation.

Table 3. GA, CS, and MCS parameters implemented for the controller design.

S. no.	GA parameters		CS parameters		MCS arameters
1	Population size	90	No. of nests	75	65
2	No. of generations	40	No. of generations	33	25
3	No. of variables	03	No. of variables	03	03
4	Selection operator	Roulette wheel	Worst nests' probability (Px)	0.22	Given in Tables 4 and 6
5	Cross over type and probability	Uniform crossover and 0.95	Step size (α)	0.9	Given in Tables 4 and 6
6	Mutation probability	0.10	Levy flight (λ)	2.4	3.3
7	Generation gap (replacement)	0.80			
8	Termination method	Maximum generations	Termination method	Maximum generations	Maximum generations

Table 4 provides the computed optimal parameters obtained from the 3 controller designs. The eigenvalues of the weakly damped eigenvalues for the MCSPDC are given in Table 4. The real parts of these eigenvalues are well placed in stable locations in the s plane, leading to stable conditions. The damping ratios are computed for the weakly damped oscillatory eigenvalues for the Case A and Case B operating conditions and are listed in Table 5. The computed damping ratios for the MCSPSDC are positive and even greater than the damping threshold ($(\xi_T) = 0.2$) selected in this paper.

Table 4. Optimal MCS-based controller parameters for 3-machine test system.

S. no.	Operating conditions (p.u.)	Gen	Optimal damping controller parameters and MCS parameters (Ks, T_1, T_2, Px, α)			Closed-loop weakly damped eigenvalues of the proposed MCSPSDC
			Gain Ks	Time constants T_1 and T_2	Px , α	
1	Case A (with S_A model)	G_2	33.412	0.2210, 0.1401	0.32, 0.18	−3.915 ± j 8.095
		G_3	47.914	0.1933, 0.3034	0.19, 0.48	−3.715 ± j 18.814
2	Case B (with S_B model)	G_2	24.099	0.3300, 0.1919	0.21, 0.35	−2.500 ± j 7.615
		G_3	39.785	0.4022, 0.1834	0.34, 0.27	−4.414 ± j 18.013

5.3. Comparison with existing standard results

Apart from comparing the damping performance of the proposed MCSPSDC with the GAPSDC and CSPSDC, the closed-loop results are also compared with existing standard results. The standard results refer to the simulation results in [26], where the genetic local search algorithm was implemented for both 3-machine and 10-machine test power systems.

From Table 5, it is clear that the damping ratios of the proposed MCSPSDC are better in comparison with the existing standard results and the other 2 controllers implemented in this paper. This satisfies the objective J_A formulated in this paper for stability. Nonlinear time domain simulations are performed and the speed deviation and power angle responses are given in Figures 11–13 for the Case A and Case B operating conditions. These deviation responses indicate that the deviations are damped at various intervals for the

different controller implementations. Comparatively, the damping performance of the proposed MCS-based controller is better than those of the GA-based and CS-based controllers. The oscillation overshoots are reduced and the deviations settle more quickly, comparatively. This satisfies the objective J_B, formulated in this paper for stability.

Table 5. Computed damping ratios for the 3-machine test system.

S. no.	Operating conditions (p.u.)	Gen	Damping ratios of the weakly damped electromechanical mode eigenvalues; damping ratio threshold (ξ_T) = 0.2			
			GAPSDC	CSPSDC	Existing standard results	MCSPSDC
1	Case A (with S_A model)	G_2	0.137622	0.201769	0.416546	0.435386
		G_3	0.092770	0.135487	0.192760	0.193719
2	Case B (with S_B model)	G_2	0.292337	0.229023	0.301734	0.311920
		G_3	0.077912	0.187935	0.209164	0.238004

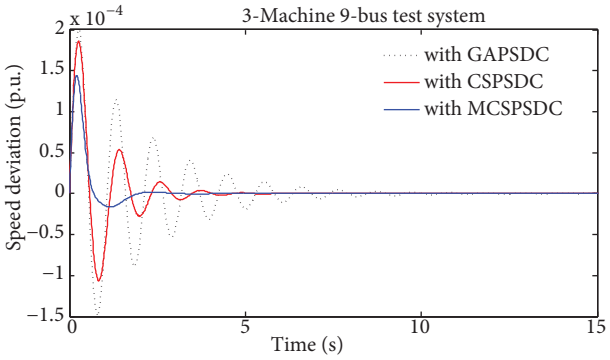

Figure 11. Speed deviation responses of the system for Case A conditions.

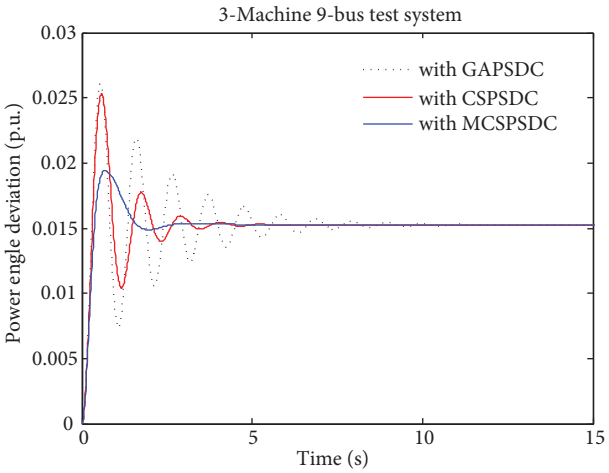

Figure 12. Power angle deviation responses of the system for Case A conditions.

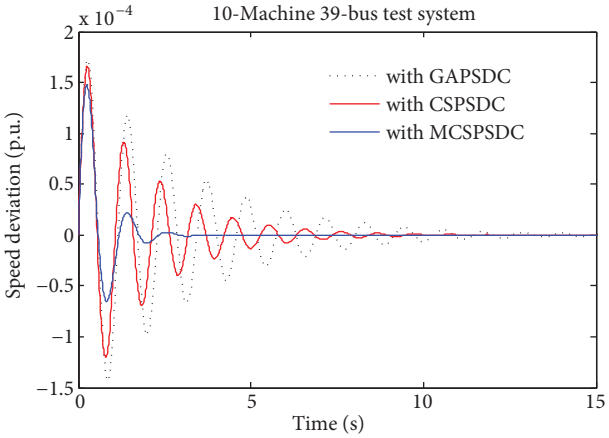

Figure 13. Speed deviation responses of the system for Case B conditions.

5.4. Ten-machine 39-bus system results

In the simulation of the 10-machine test power system, the damping controllers are implemented in all of the generators, except for generator 1. The damping performance of the controllers are analyzed for 2 conditions, namely the outage of lines 21–22 with a load change disturbance and the outage of lines 14–15 with load change disturbances.

Table 6 provides the optimal parameters computed for the 3 controller designs as well as the eigenvalues of the weakly damped modes. Table 7 provides the closed-loop damping ratios computed for the GAPSDC, CSPSDC, and MCSPSDC. The damping ratios for the MCSPSDC are better in comparison to the existing standard results [26] and compared to the damping ratios computed from the GAPSDC and CSPSDC.

Table 6. Optimal MCS-based controller parameters for the 10-machine test system.

S. no.	Operating conditions (p.u.)	Gen	Optimal damping controller parameters and MCS parameters (Ks, T_1, T_2, Px, α)			Closed-loop weakly damped eigenvalues of the proposed MCSPSDC
			Gain Ks	Time constants T_1 and T_2	Px, α	
1	Outage of lines 21–22 with ΔPd = 0.01 p.u., S_A model	G_2	37.123	0.4922, 0.2889	0.32, 0.18	–0.215 ± j 5.501
		G_3	25.342	0.1984, 0.3672	0.23, 0.27	–0.133 ± j 4.009
		G_4	64.209	0.8009, 0.2894	0.13, 0.42	–0.081 ± j 6.152
		G_5	61.329	0.1449, 0.3459	0.49, 0.09	–0.041 ± j 8.553
		G_6	18.104	0.3771, 0.7701	0.38, 0.31	–0.9915 ± j 7.9917
		G_7	17.293	0.1784, 0.6692	0.5, 0.19	–0.9399 ± j 6.571
		G_8	54.349	0.2786, 0.9287	0.29, 0.34	–0.175 ± j 9.814
		G_9	39.225	0.7801, 0.1856	0.11, 0.50	–0.199 ± j 8.015
		G_{10}	46.233	0.4509, 0.3781	0.28, 0.47	–0.3152 ± j 9.300

Table 7. Computed damping ratios for the 10-machine test system.

S. no.	Operating conditions (p.u.)	Gen	Damping ratios of the weakly damped electromechanical modes; damping ratio threshold (ξ_T) = 0.02			
			GAPSDC	CSPSDC	Existing standard results	MCSPSDC
1	Outage of lines 21–22 with ΔPd = 0.01 p.u., S_A model	G_2	0.01993	0.01154	0.034094	0.039054
		G_3	0.03299	0.03091	0.031842	0.033157
		G_4	0.00923	0.00834	0.016148	0.013165
		G_5	0.00233	0.00234	0.003300	0.004794
		G_6	0.09347	0.01293	0.012974	0.123122
		G_7	0.00878	0.01599	0.016728	0.141596
		G_8	0.01455	0.01554	0.017290	0.017829
		G_9	0.01338	0.02199	0.025308	0.024820
		G_{10}	0.02001	0.02766	0.026964	0.033873

Figures 14–17 represent the speed deviation and power angle responses computed for the 2 different operating conditions. From these deviation responses, it is clear that the proposed MCS algorithm-based

controller performs better than the other 2 controllers and in comparison with the existing standard results (results from [26]).

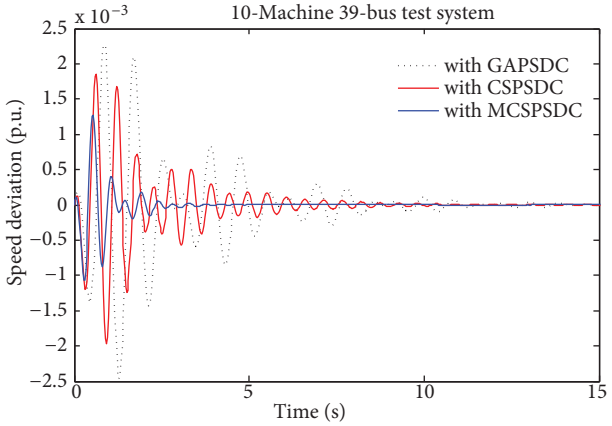

Figure 14. Speed deviation responses for the outage of lines 21–22 with 0.01 p.u. disturbance.

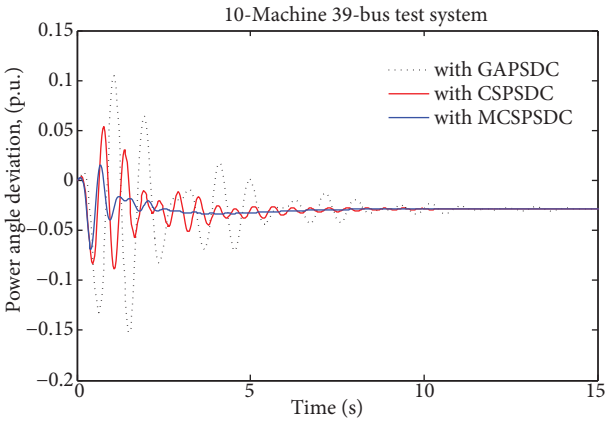

Figure 15. Power angle deviation responses for the outage of lines 21–22 with 0.01 p.u. disturbance.

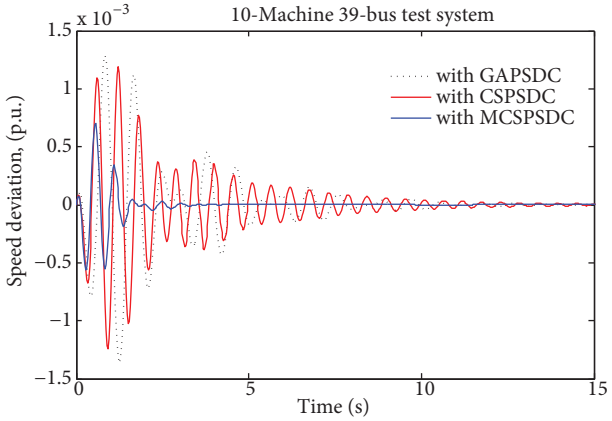

Figure 16. Speed deviation responses for the outage of lines 14–15 with 0.02 p.u. disturbance.

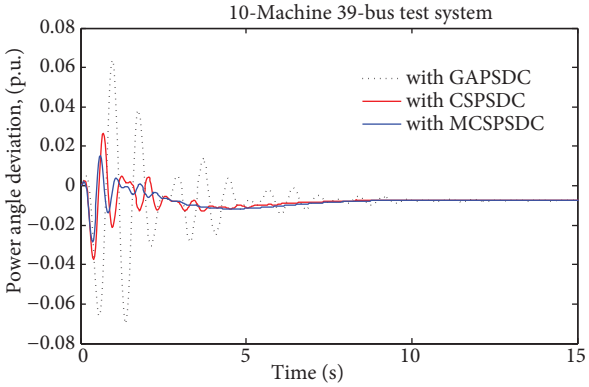

Figure 17. Power angle deviation responses for the outage of lines 14–15 with 0.02 p.u. disturbance.

6. Dominant features of the MCSPSDC

The following are the dominant features of the proposed MCS-based controller design for improving thermal power system stability.

- The closed-loop eigenvalues and damping ratios computed from the MCSPSDC design are better in terms of providing more positive damping to the oscillations compared to the GA- and CS-based controllers.
- Rotor speed and power angle deviations are damped out effectively for the MCSPSDC, comparatively.
- Optimal solution computed in fewer iterations, comparatively (as in Table 3).
- Easier implementation of the proposed MCS algorithm with only a few parameters to adjust to compute the optimal solution.

- Both torsional mode and intra mode of the oscillations experienced in the thermal power system are mitigated effectively for better stability.

7. Conclusion

This paper provides an effective and robust solution to the problem of low-frequency inertial oscillations experienced in the various configurations of 2 multimachine test power systems. The detailed comparative stability analyses (based on closed-loop eigenvalues, damping ratios, and error deviations) reveal that the proposed MCS algorithm-based controller is the best damping controller and can enhance the stability of multimachine thermal systems effectively compared to the damping performances of the GA and CS algorithm-based controller designs.

A. Appendix

Generator 1: 125 MVA, 13.8 KV, 3600 rev/min, power factor = 0.9, frequency = 50 Hz, X_d = 1.05, X_d' = 0.3, Xq = 0.686, Xq' = 0.696, Tdo' = 6.170, D = 0, M = 10.

Generator 2: 192 MVA, 18 KV, 3600 rev/min, power factor = 0.9, frequency = 50 Hz, X_d = 0.8958, X_d' = 0.1198, Xq = 0.8645, Xq' = 0.1969, T_{do}' = 6, D = 0, M = 12.8.

Generator 3: 100 MVA, 13.8KV, 3600 rev/min, power factor = 0.9, frequency = 50 Hz, Xd = 1.3125, Xd' = 0.1813, Xq = 1.2578, Xq' = 0.25, T_{do}' = 5.89, D = 0, M = 6.02.

Excitation system:

IEEE ST1A type: K_A = 210,T_A = 0.04, K_F = 0.06, T_F = 1, V_{RMax} = 6.45, V_{RMIN} = –6.0, K_E = 1, T_E = 0.

IEEE type 1 model: K_A = 190, T_A = 0.04, K_F = 0.06, T_F = 1, V_{RMax} = 6.43, V_{RMIN} = –6.0, K_E = 1.10, T_E = 0.45.

Thermal reheat and nonreheat governor turbine:

T_G = 0.2 s, R_P = 0.05, T_{RH} = 6 s, T_T = 0.3 s, F_{HP} = 0.3.

PSDC: Ks - [1 to 75], T_1 - [0.1 to 1], T_2 - [0.1 to 1], $T_1 = T_3$ and $T_2 = T_4$ (identical compensation block), Tw = 15s.

MCS parameter limits: Px - (min = 0.001 to max =1), α-(min = 0.01 to max = 0.6).

All of the parameters are in p.u., unless specified otherwise.

(2) IEEE 10-machine 39-bus system data

Data from [17].

B. Appendix

Nomenclature

PSDC	Power system damping controller (PSDC)
GAPSDC	Genetic algorithm-based PSDC
CSPSDC	Cuckoo search-based PSDC
MCSPSDC	Modified cuckoo search-based PSDC
ESS	Excitation system stabilizer
ξ	System damping ratio
$\Delta\omega, \Delta\delta$	Incremental change in the rotor speed and power angle
ΔEq'	Incremental change in the generator voltage
ΔE_{FD}	Incremental change in the generator field voltage
ΔV_R	Incremental change in the amplified voltage
ΔV_E	Incremental change in the excitation stabilizer output voltage
K_F,T_F	Gain and time constant of the excitation system stabilizer

Ke,Te	Gain and time constant of the exciter	K_1-K_6	K constants involved in the Heffron–Phillips generator model
K_A, T_A	Gain and time constant of the amplifier		
T_{do}'	Field open-circuit time constant	R_P	Steady-state speed droop

References

[1] E.R. Anarmarzi, M.R. Feyzi, M.T. Hagh, "Hierarchical fuzzy controller applied to multiinput power system stabilizer", Turkish Journal of Electrical & Computer Sciences, Vol. 18, pp. 541–552, 2010.

[2] A.D. Falehi, M. Rostami, A. Doroudi, "Optimization and coordination of SVC-based supplementary controllers and PSSs to improve power system stability using a genetic algorithm", Turkish Journal of Electrical & Computer Sciences, Vol. 20, pp. 639–654, 2012.

[3] H. Yassami, A. Darabi, S.M.R. Rafiei, "Power system stabilizer design using Pareto multiobjective optimization approach", Electric Power Systems Research, Vol. 80, pp. 838–846, 2010.

[4] M.J. Gibbard, "Robust design of fixed-parameter power system stabilizers over a wide range of operating conditions", IEEE Transactions on Power Systems, Vol. 16, pp. 794–800, 1991.

[5] P. Gahinet, P. Apkarian, "A linear matrix inequality approach to H∞ control", International Journal of Robust and Nonlinear Control, Vol. 4, pp. 421–448, 1994.

[6] M.A. Abido, Y.L.A. Magid, "Adaptive tuning of power system stabilizers using radial basis function networks", Electric Power Systems Research, Vol. 49, pp. 21–29, 1999.

[7] N. Hosseinzadeh, A. Kalam, "A hierarchical neural network adaptive power system stabilizer", International Journal of Power and Energy Systems, Vol. 19, pp. 28–33, 1999.

[8] J.A.L. Barreiros, A.M.D. Ferreira, "A neural power system stabilizer trained using local linear controllers in a gain scheduling scheme", International Journal of Electrical Power and Energy Systems, Vol. 27, pp. 473–479, 2005.

[9] A.L. Elshafei, K.A. El-Metwally, A.A. Shaltout, "A variable structure fuzzy logic stabilizer for single and multimachine power systems", Control Engineering Practice, Vol. 13, pp. 413–423, 2005.

[10] M. Abido, "Pole placement technique for PSS and TCSC-based stabilizer design using simulated annealing", International Journal of Electrical Power and Energy Systems, Vol. 22, pp. 534–554, 2000.

[11] M.A. Abido, Y.L.A. Magid, "Optimal design of PSS using evolutionary programming", IEEE Transactions on Energy Conversion", Vol. 17, pp. 429–436, 2002.

[12] H. Shayeghi, A. Safari, H.A. Shayanfar, "Multimachine power system stabilizers design using PSO algorithm", International Journal of Electrical Power and Energy Systems, Vol. 1, pp. 226–233, 2008.

[13] M. Nayeripour, M.R. Narimani, T. Niknan, "Application of modified shuffled frog leaping algorithm on optimal power flow incorporating unified power flow controller", International Journal of Modeling and Optimization, Vol. 1, pp. 191–198, 2011.

[14] X.S. Yang, Nature-Inspired Metaheuristic Algorithms, Bristol, UK, Luniver Press, 2008.

[15] P. Civicioglu, "Transforming geocentric Cartesian coordinates to geodetic coordinates by using differential search algorithm", Computers & Geosciences, Vol. 46, pp. 229–247, 2012.

[16] B. Pal, B. Chaudhuri, Robust Control in Power Systems, New York, NY, USA, Springer Science, 2005.

[17] M.A. Pai, Energy Function Analysis for Power System Stability, Norwell, MA, USA, Kluwer Academic Publishers, 1989.

[18] J. Machowski, J. Bialek, J.R Bumby, Power System Dynamics: Stability and Control, Chichester, UK, Wiley, 2008.

[19] X.S. Yang, S. Deb, "Cuckoo search via levy flights", Proceedings of the World Congress on Nature and Biologically Inspired Computing, pp. 210–214, 2009.

[20] X.S. Yang, S. Deb, "Engineering optimization by cuckoo search", International Journal of Mathematical Modelling and Numerical Optimization, Vol. 1, pp. 330–343, 2010.

[21] E. Valian, S. Mohanna, S. Tavokoli, "Improved cuckoo search algorithm for global optimization", International Journal of Communications and Information Technology, Vol. 1, pp. 31–44, 2011.

[22] X.S. Yang, Engineering Optimization: An Introduction with Metaheuristic Applications, Chichester, UK, Wiley, 2010.

[23] Y.L.A. Magid, M.A. Abido, "Optimal multiobjective design of robust power system stabilizers using genetic algorithms", IEEE Transactions on Power Systems, Vol. 18, pp. 1125–1131, 2003.

[24] S. Panda, C. Ardil, "Real coded genetic algorithm for robust power system stabilizer design", International Journal of Electrical, Computer and System Engineering, Vol. 2, pp. 6–14, 2008.

[25] Z. Wang, C.Y. Chung, K.P. Wong, D. Gan, Y. Xue, "Probabilistic power system stabilizer design with consideration of optimal siting using recursive genetic algorithm", European Transactions on Electrical Power, Vol. 21, pp. 1409–1424, 2011.

[26] M.A. Abido, "Parameter optimization of multimachine power system stabilizers using genetic local search", Electrical Power and Energy Systems, Vol. 23, pp. 785–794, 2001.